Hindawi
International Journal of Polymer Science
Volume 2022, Article ID 6372264, 18 pages
https://doi.org/10.1155/2022/6372264

Research Article

Oil Palm Empty Fruit Bunch (OPEFB) Fiber-Reinforced Acrylic Thermoplastic Composites: Effect of Salt Fog Aging on Tensile, Spectrophotometric, and Thermogravimetric Properties

Vladimir Valle,[1] **Alex Aguilar**,[1] **Jeronimo Kreiker**,[2] **Belén Raggiotti**,[3] **and Francisco Cadena**[1]

[1]*Departamento de Ciencias de Alimentos y Biotecnología, Facultad de Ingeniería Química y Agroindustrial, Escuela Politécnica Nacional, Quito, Ecuador*
[2]*Centro Experimental de la Vivienda Económica (CEVE)-CONICET, AVE., Igualdad, 3585 Córdoba, Argentina*
[3]*Centro de Investigación, Desarrollo y Transferencia de Materiales y Calidad (CINTEMAC), UTN-FRC, Maestro M. Lopez y Cruz Roja Argentina, Córdoba, Argentina*

Correspondence should be addressed to Vladimir Valle; vladimir.valle@epn.edu.ec

Received 6 February 2022; Accepted 15 March 2022; Published 15 April 2022

Academic Editor: Marta Fern ndez Garc a

The prioritization of agroindustry fiber wastes as raw materials in development of composites has become a challenge to obtain higher value-added products with targeted applications. In this study, natural fiber-reinforced polymer matrix composites were elaborated using two fiber sizes (605 μm and 633 μm) of oil palm empty fruit bunch (OPEFB) and acrylic thermoplastic resin. In doing so, resin and fibers were mixed at room temperature by maintaining filler content of 42 wt. % for all formulations. In addition, thermomechanical compression moulding was used as composite manufacturing process at four processing temperatures (80, 100, 120, and 140°C). All formulations were subsequently exposed to salt fog spray aging for 330 hours. The effects of accelerated aging process on mechanical, spectrophotometric, and thermogravimetric characteristics were studied. On the whole, results have shown feasibility to use a facile method to elaborate composites based on waterborne acrylic matrix and OPEFB fibers. After salt spray testing, it was observed detectable levels of *Aspergillus* spp. of fungi in all samples, as a result of phylogenetic organization of microbial activity. Tensile behavior of composites was significantly influenced by processing temperature and fiber size. In broad terms, their overall mechanical properties were improved by the increase of temperature. Additionally, infrared spectroscopy results showed important bands mainly associated to biodegradation of cellulose, hemicellulose, and lignin. On the other hand, two degradation stages were mainly identified in thermogravimetric evaluation. Noteworthy, aging had no significant effect on the thermal properties of composites.

1. Introduction

The application of natural fibers as reinforcement in polymer matrices has expanded during the last decade in several industry sectors. Looking towards a sustainable development, it is desirable the prioritization of agroindustry wastes as raw materials in development of eco-friendly, high-productivity, and cost-effective composites [1, 2]. Encouraged by circular economy approach, the use of oil palm empty fruit bunch (OPEFB) wastes constitutes an interesting challenge to obtain higher value-added products with specific applications. In this respect, several researchers have attempted to improve physical and chemical properties of composites based on OPEFB fibers in various polymer matrices [1, 3–10]. Even though many studies regarding the effects of lignocellulosic fiber characteristics on the properties of polymer matrix composites have been conducted, investigations based on different OPEFB fiber sizes and processing temperatures have not been broadly described in the literature.

Composite materials reinforced with natural fibers are usually affected by their susceptibility to environmental degradation. Both polymers and natural fibers react

differently to changes in environmental factors and mechanical solicitations. Particularly, an important setback of natural fibers is relatively poor in its mechanical integrity due to vulnerability to moisture absorption. Furthermore, it is often noted that chloride-containing salt of coastal climates is an important parameter affecting properties of these composite materials. Thus, the performance of fiber reinforced polymer matrix composites—under extreme salty conditions—becomes highly important because chloride levels as well as rate of absorption and desorption of natural fibers in wet-dry cycles have significant influence on the durability of the composites [11, 12].

There are many polymeric matrices extensively used in the industry to meet high performance requirements; in particular, acrylic is an exceptionally versatile polymer due to a wide range of properties, which can be achieved by carefully selecting appropriate combinations of monomers. Copolymers of acrylate and methacrylate exhibit desired balanced between hardness and flexibility. Toughness, hydrolysis resistance, and low absorption of high-energy ultraviolet portion make acrylic polymers suitable for applications requiring good weathering resistance [13]. In recent years, numerous studies have employed acrylic matrix in composite fabrication with glass fibers [14–17], carbon fibers [18–20], metal fiber [21, 22], polyethylene fibers [23, 24], rayon fibers [25], and hybrid fibers [26]. Other researches have narrowly dealt with natural fibers like flax [12, 27], jute [28, 29], ramie [30], hemp [31], and wood [32]. Notwithstanding, there is a research gap on the use of OPEFB fibers as reinforcement in acrylic matrix composite development.

Acrylic emulsion polymers have traditionally been used as binders for general purpose in architectural and industrial coatings due to color stability and transparency [33]. The elaboration of acrylic latexes involves monomer emulsification following by water phase polymerization. Unlike in thermosetting acrylic resins, which involve oxidizing or cross-linking reactions, acrylic emulsions were devised not only to form films with solvent evaporation but also to be fast-drying [13]. Low-cost and relatively simple technologies are of paramount significance in industrial sectors that produce mature and conventional standard products. In constructive applications, for example, this requirement can be fulfilled by waterborne polymers.

From the perspective of fiber-reinforced composite manufacturing, literature has reported several fabrication techniques, namely, injection moulding, compression moulding, resin transfer moulding, extrusion, melt electrospinning, filament winding, and vacuum infusion. The latter provides a high-quality alternative to develop composites at room temperature by using liquid thermoplastic resins [2]. Nevertheless, vacuum infusion has some limitations in terms of application range. Aside from a successful vacuum bagging system requirement, this technique implicates higher consumable costs and relatively slower cycle times [34, 35]. Systematic investigations have also revealed that processing temperature shows critical effects on final properties of composite materials. In this regard, the influence of temperature on the viscosity of the polymeric matrix must be considered as one of the main processing parameters that modify the interfacial interactions between fibers and matrix [27–29].

On the other hand, aging evaluation has been frequently used in paint and coating development to mainly simulate outdoor exposure degradation. There are several highly specialized methods including elements like sunlight, moisture, temperature, oxygen, and chemical exposure. However, salt spray test plays a very major role to mimic saline habitats of coastal regions, hypersaline lakes, solar salterns, and other salinity stress environments produced by anthropogenic activities [13, 36]. Therefore, accelerated testing methods can be also useful options to simulate, as closely as possible, the aging of composites in specific environments in a much shorter time. Herein, the study is aimed at elaborating OPEFB fiber-reinforced acrylic thermoplastic composites by means of a facile method and subsequently studying the effect of salt fog atmosphere on their mechanical, spectrophotometric, and thermogravimetric characteristics. The influence of both fiber size and processing temperature over composite behavior under accelerating test was particularly investigated.

2. Materials and Methods

2.1. Materials. Liquid acrylic thermoplastic resin SINTACRIL A-292® was purchased from Poliacrilart (Quito, Ecuador). The resin was waterborne formulated by copolymers of acrylate and methacrylate with 42 wt. % solid content. Its Brookfield viscosity (SP1, 12 rpm) and density (25°C) were 0.07 Pa·s and 1.06 ± 0.01 g/cm^3, respectively. OPEFB wastes used in this study and consisting of about 46% of cellulose, 24% of lignin, and 3% of extractive [37] were supplied by a local company specializing in oil palm production.

2.2. Elaboration of OPEFB/Acrylic Thermoplastic Composites

2.2.1. Preparation of Composites. OPEFB wastes were initially dried under sunlight for 24 h and then milled through a blade milling machine SHINI, model SG-2348E (Ningbo, China). The resulting OPEFB fibers were sieved to obtain two fiber sizes. In order to eliminate the influence of outliers on the tails of fiber size distribution, the actual average sizes were obtained from a robust statistical method of central tendency by means of trimmed-mean estimator. To do so, two hundred fibers per size were measured using a stereomicroscope MEIJI TECHNO, model EMZ-13TR (Saitama, Japan). The acquisition and processing of the images were performed with the TCapture software. The trimmed-mean values of fibers sizes were 605 μm and 633 μm.

OPEFB/acrylic thermoplastic composites were separately formulated with the two fiber sizes obtained in OPEFB conditioning. An appropriate proportion of resin and fibers were mixed at room temperature, using mechanical stirrer at 500 rpm for 30 min. After, specimens were processed using a compression moulding machine LAB TECH, model LP-S-50 (Mueang Samut Prakan, Thailand), at four temperatures: 80, 100, 120, and 140°C, under a pressure of 150 bar for 40 min. The processing temperatures were selected based on the thermal stability of raw materials. It should be also indicated that composite was performed with the highest content of OPEFB fiber obtaining through the elaboration method aforementioned. As such, all samples were prepared

by maintaining 42 wt. % and 58 wt. % of filler content and matrix, respectively. Figure 1 shows the schematic representation of the experimental procedure.

2.2.2. Characterization. Mechanical evaluation, regarding tensile modulus, tensile strength, elongation at break, and toughness, was accomplished by the use of a universal testing machine INSTRON, model 3365 (Norwood, USA), in accordance with standard ASTM D 638, with load cell of 500 N and crosshead speed of 20 mm/min. The mean values of tensile results were determined from ten test specimens for each composite formulation. Moreover, Fourier transform infrared spectroscopy (FTIR) in attenuated total reflection mode was performed by using a spectrometer JASCO, model FT/IR-C800 (Tokyo, Japan), from 4000 to 600 cm^{-1} with a resolution of 4 cm^{-1} and 20 scans. In addition, thermogravimetric analysis (TGA) was carried out using a thermobalance SHIMADZU, model TGA-50 (Kyoto, Japan), from 20°C to 600°C with heating rate and nitrogen flow of 10°C/min and 50 mL/min, respectively. The morphology of composites was complementarily evaluated by scanning electron microscopy (SEM) with electron microscope ASPEX, model PSEM eXpress (Billerica, USA), under 20 kV of accelerating voltage.

2.3. Salt Spray Testing. Aiming towards simulating critical salty environmental circumstances, OPEFB/acrylic thermoplastic composite samples measuring 250 mm × 250 mm × 2 mm were exposed to a controlled salt spray atmosphere. The test was performed in a chamber Q-FOG, model CCT600 (Cleveland, USA), based on the protocol of ASTM B117. Samples were exposed to a direct and continued salt fog of 6 wt. % sodium chloride aqueous solution at 35 ± 1 °C. After 330 hours of exposition, when a notable deterioration of the material surface was observed, specimens were removed from the testing chamber. To further understand the influence of salt fog spray aging over composite performance, exposed samples were analyzed in terms of their mechanical, infrared, thermal, and morphological characteristics according to the set of conditions described in the previous section.

After aging evaluation, a qualitative microbiological analysis was performed. In doing so, fungi were isolated from different areas of the composite samples. Two-gram sample was dissolved in 100 mL of sterilized distilled water. After three serial dilutions, 100 μL of this diluted sample was then transferred to petri plates containing potato dextrose agar (PDA). Afterward, petri plates were then placed at 25°C for 3–10 days. Fungal colonies were transferred into PDA slants and incubated for 7–30 days, after which their genera were determined on macromorphology criteria.

3. Results and Discussion

Overall properties of composites depend on compatibility between fiber and matrix [38, 39]. Adhesion and nature of bonding of composite elements are determined by various aspects, chiefly of diffusivity of element materials and morphological properties of natural fibers [40]. From the imbibing process, OPEFB fibers were completely covered by the acrylic thermoplastic matrix, as shown in Figures 2 (a) and 2(b). Taking into account porous surface of OPEFB fibers, it can be seen that the polymer matrix was also covering superficial parts of micropores. As a result of processing molding, there were obtained composites with relatively homogeneous surface. Figures 2(c) and 2(d) present images of composites before salt spray testing.

From Figure 3(a), it could be seen that after 330 hours of exposition to controlled salt fog atmosphere, the surfaces of the composites showed fungal presence. In the light of the results presented in Figure 3(b), morphological identification evidenced detectable levels of *Aspergillus* spp. On review of different researches related to environmental conditions for fungi growth, some genera are easy adaptable to humid climate and can survive at hypersaline environment of sodium chloride. It is however worthy of note that edaphoclimatic conditions of OPEFB wastes could generate several microbial diversities, including fungi and bacteria. Numerous phylogenetically unrelated fungi have been reported to grow in salty water with high concentration of sodium chloride [41–43]. From the perspective of lignocellulose biodegradation, fungi are the predominant decomposers of cellulose and hemicellulose by means of hydrolysis reactions to form fermentable sugars whilst lignin is a macromolecule with nonfermentable phenylpropane units linked C–C and C–O–C bonds requiring high energy to break down. Nevertheless, a number of fungi usually produce lignin peroxidases, manganese peroxidases, laccase-like multicopper oxidases, and so forth [41].

Figure 4 depicts SEM micrographs of worn surfaces after salt fog atmosphere. Expectedly, during the test water and salt were absorbed by the matrix and OPEFB fibers. The absorbed moisture caused increase in microbial activity which in turn resulted in random orientation microstructural changes. In particular, biodegradation process produced significative defects like voids and microcracks in the composites; these tend to decrease with processing temperature.

3.1. Mechanical Characterization. Polymeric composites undergo a variety of stresses when being in service; therefore, inspecting the response to tensile solicitations is one of the most relevant evaluation criteria for application purposes [44]. Mechanical properties of fiber-reinforced polymer composites depend on several factors. The fiber type is, at least in principle, a critical aspect when considering tensile mechanical performance [38, 39]. In this context, the studies regarding the use of acrylic thermoplastic resins with different synthetic fibers, in particular with glass fiber and carbon fiber [45], have revealed notable improvements, both in tensile strength and modulus, compared to those obtained when the reinforcement is natural, such as flax [27, 29, 46]. The reported literature on tensile stress-strain behavior of natural fiber-reinforced acrylic thermoplastic composites has identified three distinct regions [27, 46]. The first was associated to the initial linear elastic behavior, the second to the evolution of damage with loss of stiffness (slight nonlinearity), whereas the third to the intensification of damage leading up to ultimate failure. In the study reported herein,

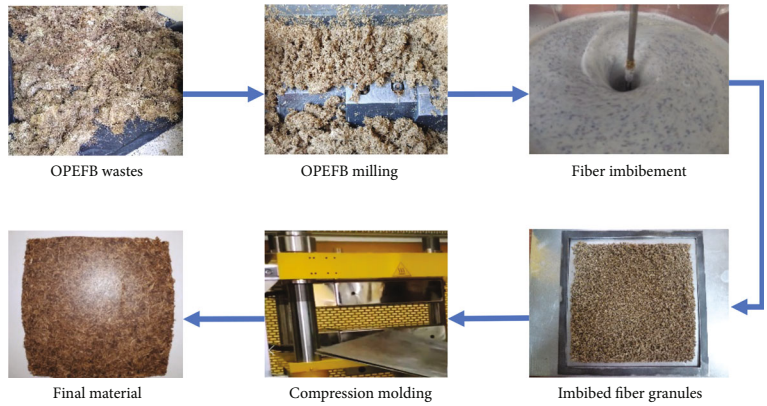

Figure 1: Experimental setup used for OPEFB/acrylic thermoplastic composite elaboration.

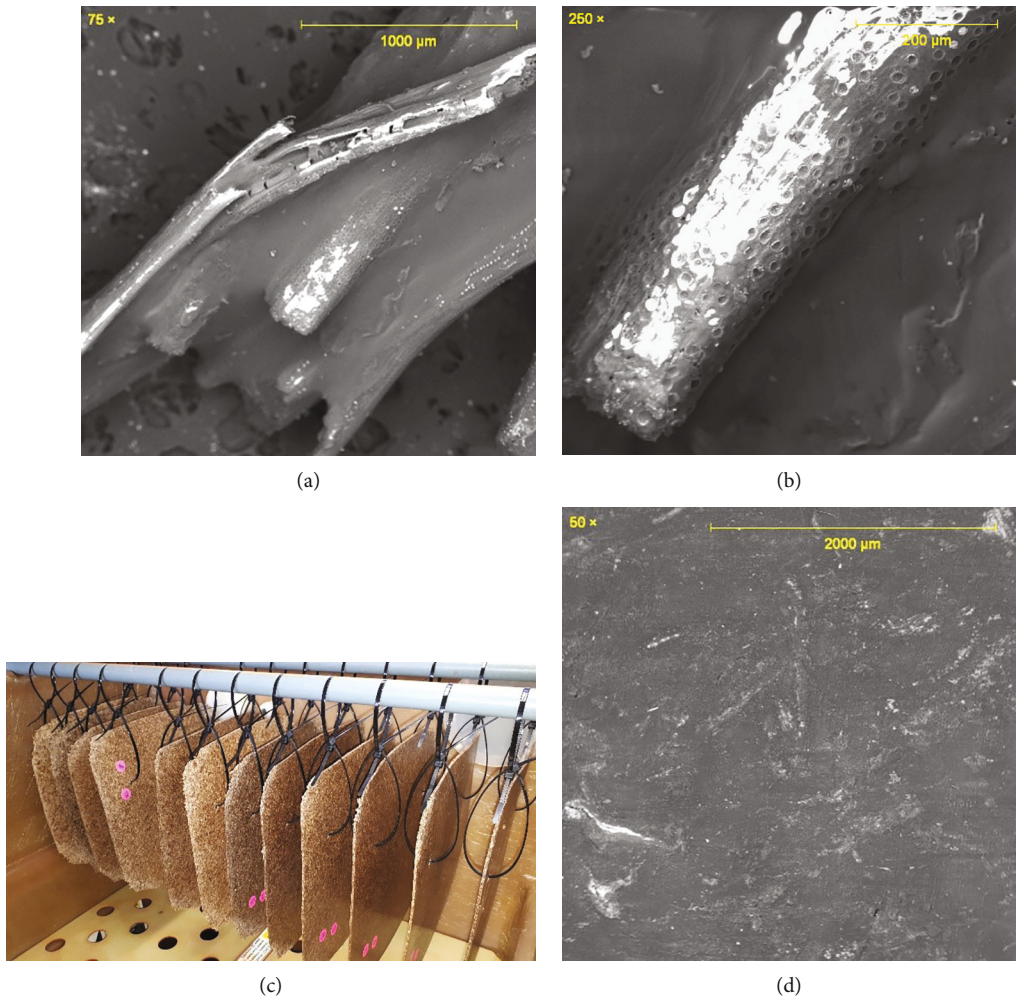

Figure 2: (a, b) SEM images of imbibed fiber granule, (c) OPEFB/acrylic thermoplastic composites before salt spray testing, and (d) SEM image of composite before salt spray testing.

overall results of tensile stress-strain showed ductile-like behavior. In all cases, noticeable plastic deformation was observed; however, the strain hardening zone was clearly higher than the necking region. Tensile stress-strain behavior of raw materials and composite is depicted in Figure 5.

Fiber loading is another relevant factor that influences tensile mechanical properties of natural fiber-reinforced polymer composites [38, 40]. A variety of polymers, modified by OPEFB fibers, have revealed that fiber content considerably affects properties of composites [47, 48]. Due

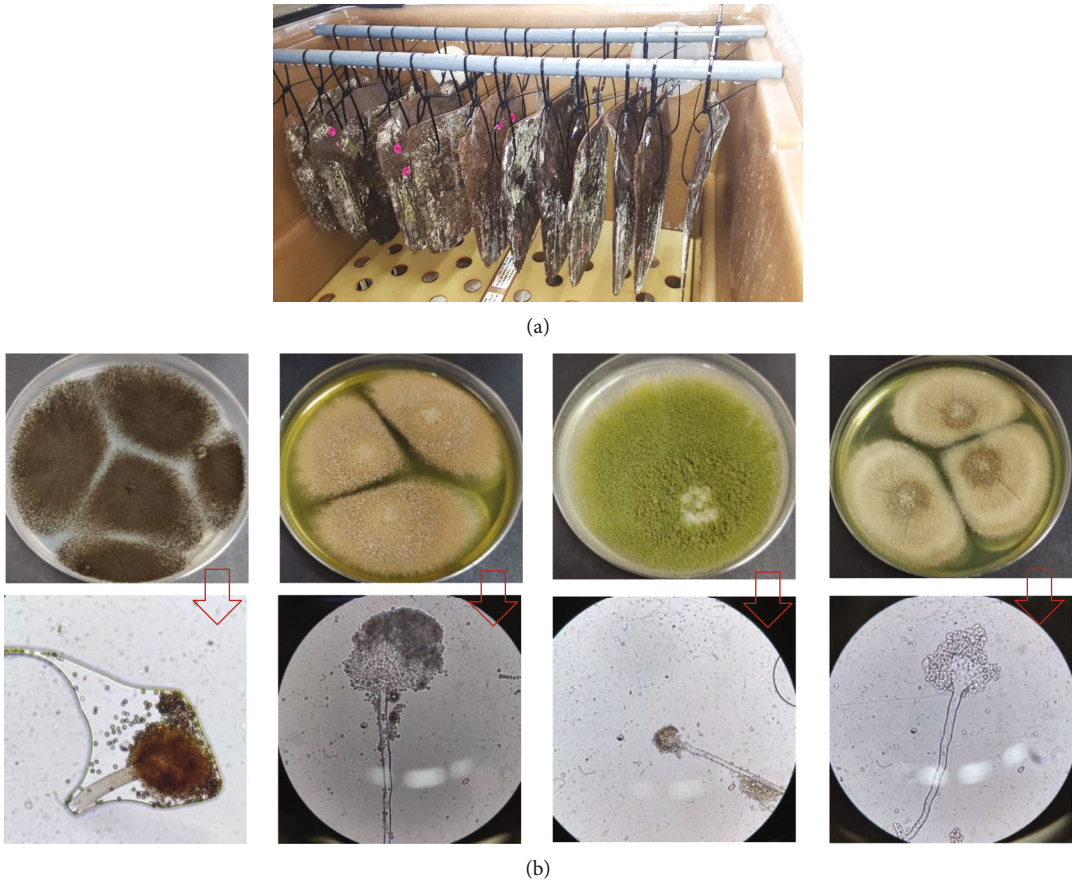

(a)

(b)

Figure 3: (a) OPEFB/acrylic thermoplastic composites after aging and (b) colony morphology of *Aspergillus* spp. observed on composite surfaces at macroscopic and microscopic (40x/0.65) scale.

to the fact that the reinforcement generally plays a dominant role over the matrix, the composite strength is proportional to the fiber strength because natural fiber is often stronger than polymer matrix [38]. The plot of Figure 5(c) shows three distinct regions in the stress-strain curve, which are in concordance with similar literature reports about natural fiber-reinforced acrylic thermoplastic composites [27, 46]. Nonetheless, it should be noted that, in those studies, the matrix used (Elium®) had different mechanical characteristics than the polymer used for our composite formulations, despite both being acrylic thermoplastic polymers. Comparing Figures 5(a)–5(c), it could be seen that the initial part of the stress-strain curve shows improvement of stiffness and strength that is probably associated to unlinear performance of OPEFB fiber reinforcement, as it has been postulated in the literature [38, 40, 49–52]. This behavior predominated in the composite due to the high load of added fibers. The second part of the stress-strain curve, Figure 5(c), P2, acquainted as a transition zone, could be associated to the beginning and propagation of failure mechanism owing to the deviation and fall of the stress-strain curve. Lastly, the third part of curve might be assigned as an intensification region of the failure mechanism during the deformation of the polymer matrix. Section marked by a decrease in composite stiffness leading up to ultimate failure [27, 38, 46].

On the other hand, Figure 6 illustrates the influence of fiber size and processing temperature over tensile behavior. It was initially observed uneven statistic dispersion among formulations; nonetheless, mechanical response of natural fiber composites is largely dependent on fiber properties, which in turn are influenced by a number of factors like size, geometry, water absorption, tendency to form aggregates, chemical composition, organic extractives, inorganic (ash) components, and different types of waxes [40, 53]. In particular, macrostructure of OPEFB fibers involves nonuniform length-to-diameter ratio, irregular shape, rugose surface, and so forth. Additionally, main morphology features include different microfibril angles, a central empty section named as lacuna as well as randomly and loosely organized network of microfibrils [47, 54]. Aforementioned characteristics join with impurity presence could be considered as natural defects leading to a distribution widely spread out from the mean. It is thus of practical significance to understand that it is neither possible to avoid relatively high dispersion in the response of OPEFB/acrylic thermoplastic composites under tensile loading.

Tensile mechanical properties of composites also depend on adhesion in terms of better compatibility between fiber and matrix [28, 38]. Even though OPEFB fibers were initially imbibed by the matrix, as shown in

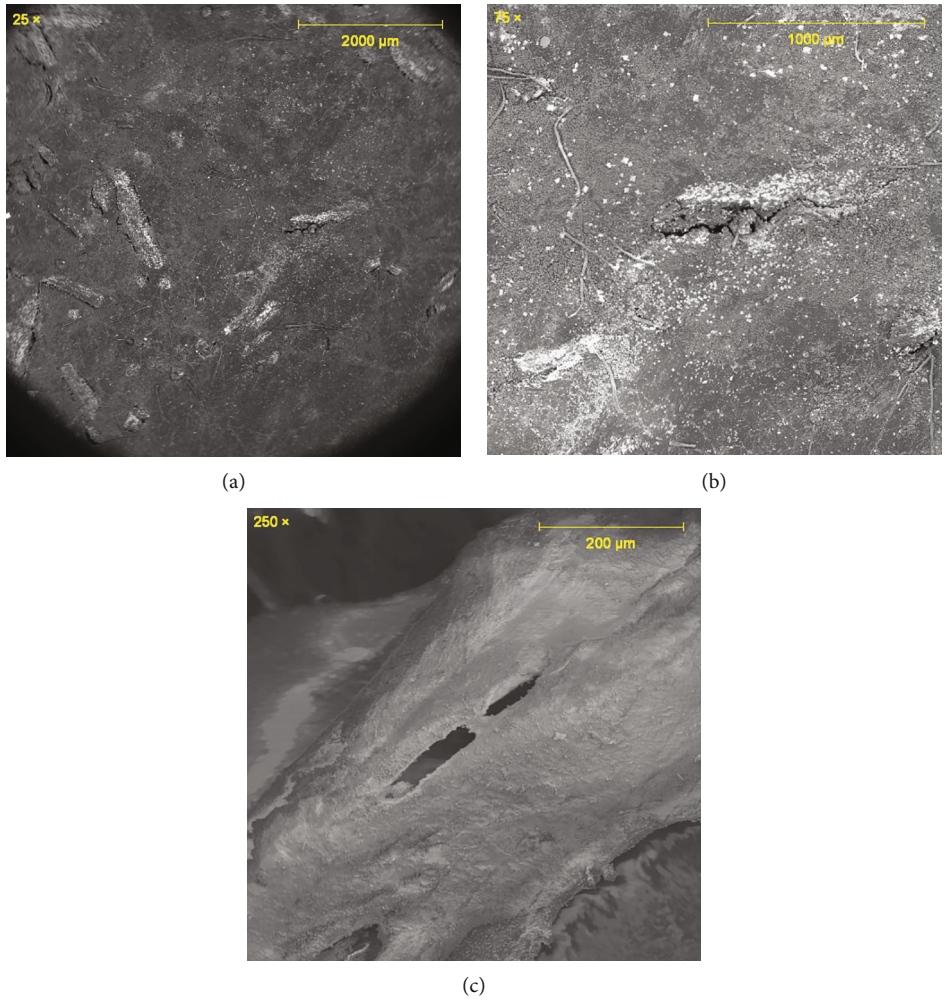

(a) (b)

(c)

Figure 4: SEM images of OPEFB/acrylic thermoplastic composites after aging.

Figures 2(a) and 2(b), acrylic microstructure typically shows porous that allows both liquids and gases diffuse through the polymer [55]. Thus, during aging test, water diffusion and further sorption by OPEFB fibers induced both differential swelling of natural fiber [12] and microorganism growth, which can be observed in the images of Figure 3(a). *Aspergillus* spp. have been reported as one of the microorganisms responsible for biodeterioration of acrylic-based polymers such as in glass fiber composites. The changes observed in the acrylic matrix due to microbiological attack were disfigurement, erosion, and loss of mechanical properties; the latter is a consequence of microcracking on the polymeric surface [56]. These structural defects were found on our composite surface after salt fog aging, as illustrated in Figure 4. In addition, stresses generated by fiber swelling at the interface level contributed to the damage and microcracking of the matrix, which intensified water absorption. Because of this fact, further degradation was probably produced by the access of free oxygen, enzymes, and free radicals which lead to weaken fiber–matrix interfacial adhesion [12]. Given these points and based on Figure 6, tensile mechanical properties were somewhat lower after salt fog spray aging except for tensile modulus, whose increment after salt fog aging demonstrates stiffness boost of the acrylic matrix.

Tensile modulus and tensile strength results are depicted in Figures 6(a) and 6(b). No specific tendencies of these properties with temperature were identified. These behaviors are possibly caused not only by random orientation and dispersion of fibers but also by some changes in mechanical response of the matrix [14, 27, 29]. Nonetheless, there was a notable decrease in both tensile parameters at 140°C that was linked to the influence of temperature on the viscosity of the polymeric matrix [29]. Indeed, results showed strengthening of modulus and slight enhancing of stress resistance along composite with increasing fiber size. In other words, longer fibers provided greater stiffness to the composite and were able to withstand stresses a little more easily. Additionally, due to the fact that composites were made with the same fiber load, there were observed slight changes in tensile strength between formulations of different fiber sizes processed at the same temperature. Tensile mechanical properties of natural fiber-reinforced polymer composites especially the tensile strength have strong relationship with

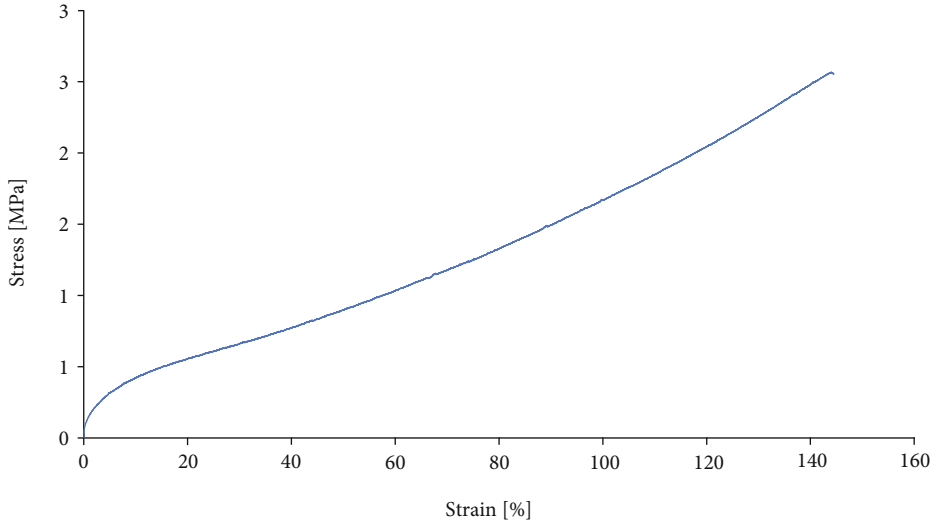

(a)

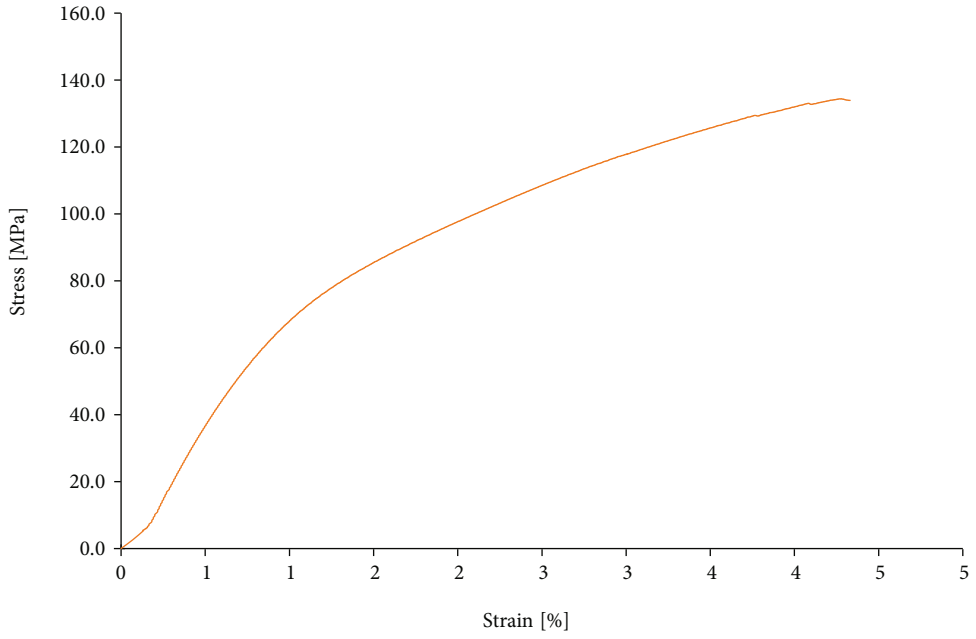

(b)

Figure 5: Continued.

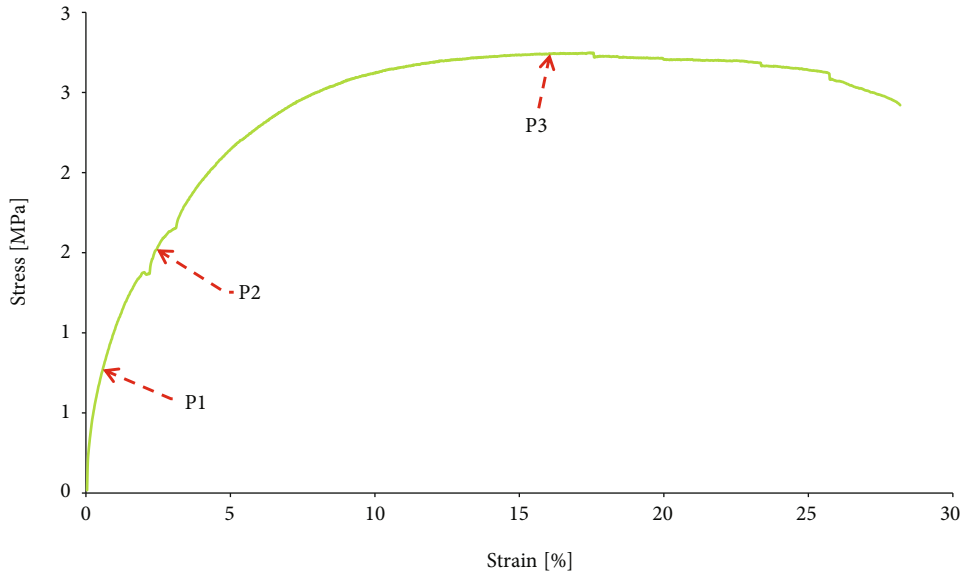

(c)

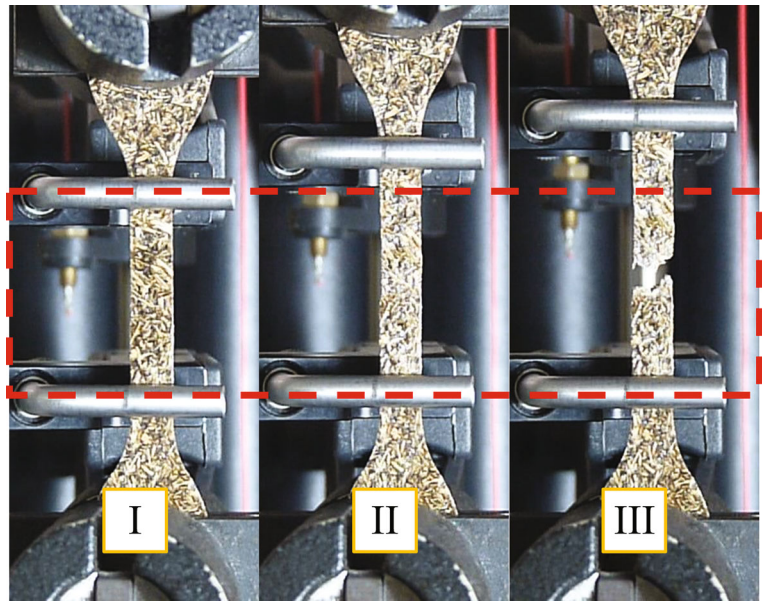

(d)

Figure 5: Tensile stress-strain behavior of (a) acrylic thermoplastic matrix, (b) OPEFB fiber, (c) OPEFB/acrylic thermoplastic composite, and (d) tensile specimen under test: (I) before, (II) during, and (III) after.

fiber volume fraction, because fibers serve as the principal load-bearing members in a composite [38–40, 49].

As can be seen in Figure 6(c), elongation at break was clearly influenced by fiber size. Considering obtained results, the increasing of fiber size weakened ultimate elongation of composites, regardless of processing temperature. Additionally, it is important to consider that the larger the fiber size, the worse the mechanical performance of natural fiber-reinforced composites [38]. This drawback was probably intensified by deficiencies in interfacial adhesion between larger OPEFB fibers and acrylic thermoplastic matrix [28, 40]. Aside from fiber size, changes on tensile characteristics were noticed as a result of processing temperature. It should be stated that the increase of processing temperature produced higher ultimate failure. Data suggest that water and organic solvents were gradually evaporated from the composite. Indeed, the temperature increase leads polymer to cover porous, lacunas, and microfibrils [27, 29]; therefore, a better compaction of the final composite at 140°C was distinguished. According to the literature, this behavior can be linked to better fiber–matrix interactions due to the fact that manufacturing parameters are main aspects to be considered in tensile performance [44, 53, 57]. Nevertheless, the only exception to the above arguments was the composite with the smallest fiber size processed at 80°C. This formulation exhibited a fracture strain similar to the highest elongation at break of all formulations, elongation showed by the composite with the same fiber size but processed at 140°C.

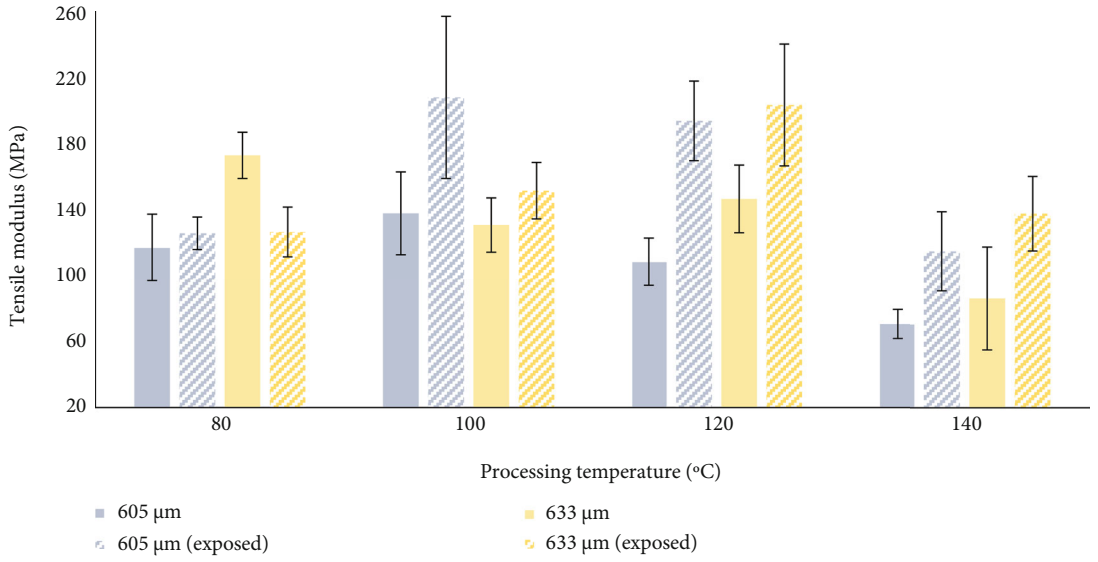

(a)

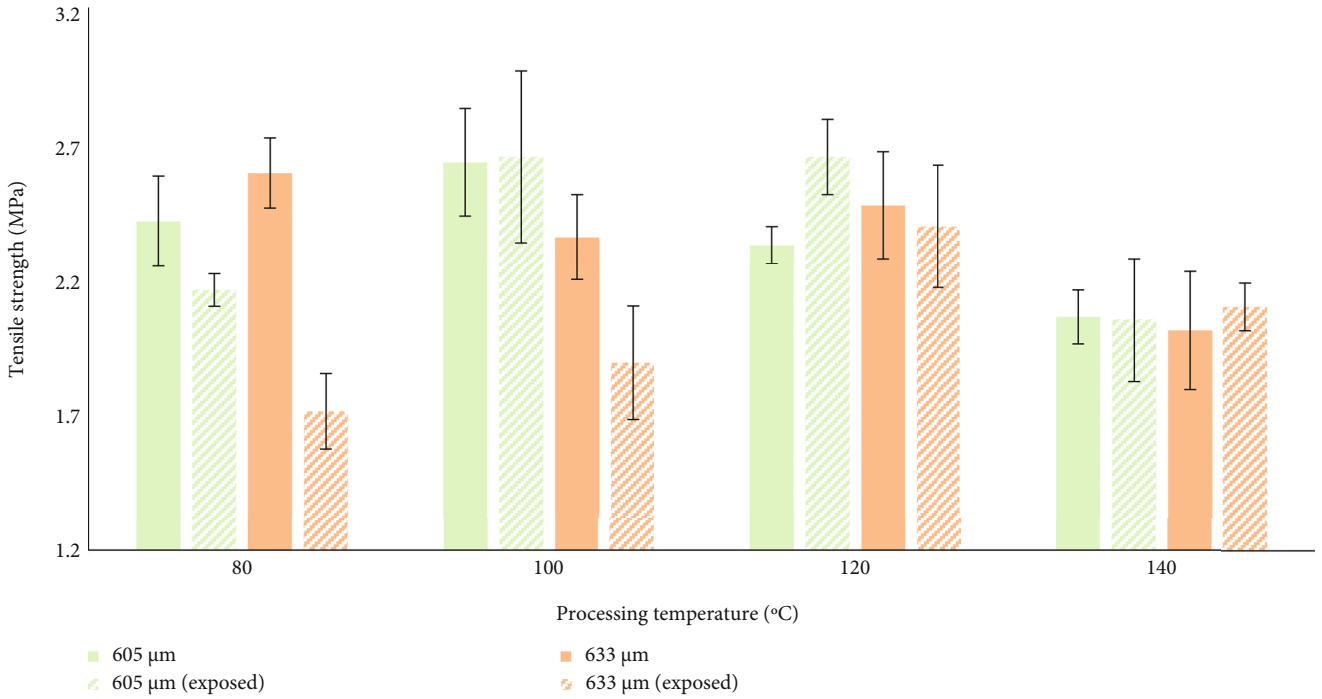

(b)

Figure 6: Continued.

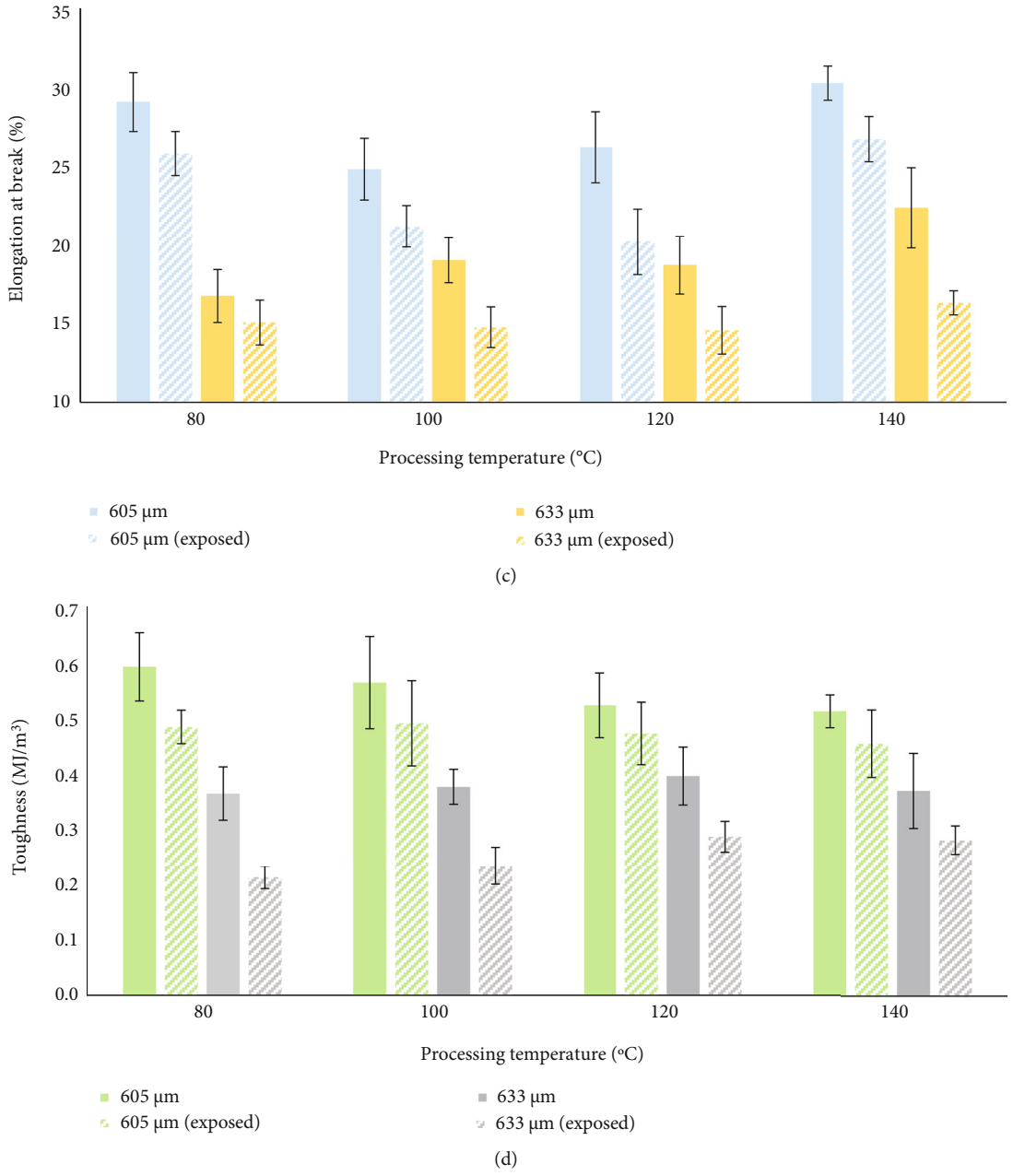

Figure 6: Tensile characteristics of OPEFB/acrylic thermoplastic composites: (a) tensile modulus, (b) tensile strength (c) elongation at break, and (d) toughness.

Hence, it is possible to infer that the effect of smaller fiber size, prior to the contribution of the increase in the processing temperature to strengthen the fiber–matrix interactions [27, 29], equated the best performance of the matrix without using a higher energy expenditure in the process.

Unlike fibers with a uniform cross section, the irregular shape and nonuniform length-to-diameter ratio of OPEFB fibers did not allow efficient stress transmission from acrylic matrix to the filler [40, 54]. This effect is higher increasing fiber size from 605 μm to 633 μm, as shown in Figure 6(d). Fibers are usually the principal load-carrying element in a composite; however, matrix also serves not only to keep fillers randomly or specific orientated but also to be a load transfer medium between them [44]. On the view of matrix response, methyl-methacrylate and acrylate proportion allowed the matrix somewhat desired balance between flexibility and toughness.

3.2. Infrared Evaluation. Once infrared spectroscopy is based on vibration modes of functional groups of molecules, the analysis of obtained results was focused mainly on spectral differences of aliphatic hydrocarbons, oxygen-containing compounds, aromatic compounds, heterocyclic compounds, and nitrogen-containing compounds molecules [58]. Figure 7 illustrates the FTIR results of raw materials, i.e., acrylic resin and OPEFB fiber. The acrylic resin spectrum

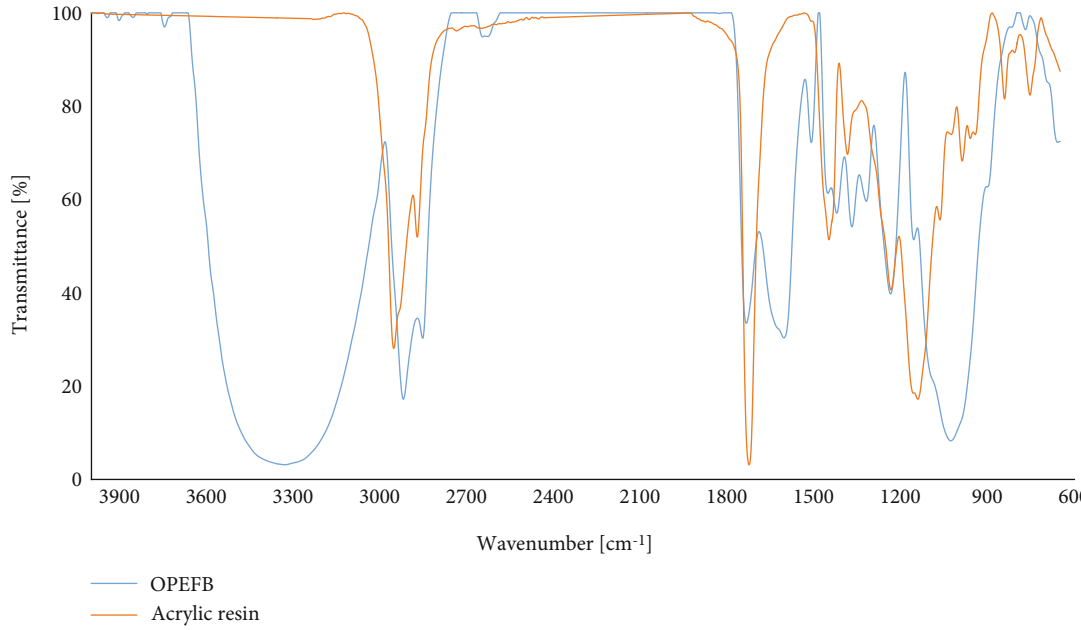

Figure 7: FTIR curves of raw materials.

resulted from the frequencies of several groups. As such, it was observed the presence of a broad band at 3360 cm^{-1} attributed to the absorption vibration of O–H group, due to waterborne nature of resin. The band of C–H stretching, associated not only to backbone chain but also to methyl substituent, was identified at 2956 cm^{-1}. The band at 1729 cm^{-1} corresponded to C=O stretching of the ester group, whereas the band at 1451 cm^{-1} was linked to the bending of O–CH_3. In addition, bands at 1386 cm^{-1} and 1238 cm^{-1} were ascribed to C–CH_3 bending and C–C–O stretching, respectively. Besides, the band at 1164 cm^{-1} corresponded to C–O–C bending [58].

As regards OPEFB, the spectrum evidenced a broad band at 3328 cm^{-1} corresponding to vibration of O–H group which was ascribed to water, alcohols, and phenol components [59–63]. The bands at 2921 cm^{-1} and 2854 cm^{-1} were associated to methylene asymmetric C–H stretching and methylene symmetric C–H stretching, respectively [63, 64]. The band at 2854 cm^{-1} was related to CH and CH_2 groups from cellulose and hemicellulose. Ester group of hemicellulose and waxes was confirmed through the band at 1735 cm^{-1}. Additionally, the presence of C–O–C stretching vibration of pyranose ring in polysaccharides was identified at 1158 cm^{-1}. Moreover, glycosidic bond was corroborated by transmittance band at 898 cm^{-1} [62]. In general, cellulose was confirmed by bands at 898, 1029, and 1158 cm^{-1}, whereas hemicellulose was identified by the presence of bands at 1029, 1234, 1319, 1371, 1421, 1735, 2921, and 3328 cm^{-1}. Furthermore, aromatic ring corresponding to lignin was observed at 1455 and 1511 cm^{-1} [60, 65].

Infrared spectra of OPEFB/acrylic thermoplastic composites are presented in Figure 8. Before salt fog test, the results showed minimal differences in infrared absorption of composites elaborated with 633 μm and 605 μm. The fiber size used in the current study did not produce significant changes in the modes of vibration of the composite molecules. On the other hand, it should be note that the increase of processing temperature not only led to a thermodynamically fast evaporation of water and solvents but also helped to coalescence of dispersed phase. However, this effect was not clearly observed in the composites before aging due to overtone bands.

According to the results presented in Figures 3 and 4, the salt fog atmosphere produced some deterioration patterns probably dominated by different biodegradation mechanisms. However, spectra could not evidence all of them, due to some drawbacks like overtone bands, Fermi resonance, and coupling. Comparing FTIR curves before and after aging, the increase of the band in the range of 3700–3000 cm^{-1} could be produced not only by the presence of O–H stretching of carboxylic acids but also to O–H from a range of phenolic compounds resulting of fungal growth [66]. However, the absorption of this group was dominated by processing temperature; specifically, the highest temperature, produced less O–H infrared absorption, due to better coalescence of the matrix. The set of the bands between 3000 cm^{-1} and 2600 cm^{-1} has been decreased due to noticeable wear of acrylic matrix as well as to the degradation of cellulose and hemicellulose. In addition, it was clearly distinguishable new bands in the range of 2500-2000 cm^{-1}, which were assigned to fungi presence. The new band at 1640 cm^{-1} was ascribed to protein C=O stretching of amide I, whereas the band at 1540 cm^{-1} was associated to C–N stretch and protein in N–H bend; according to the literature, the former bands are assigned to fungi mycotoxins [67].

3.3. Thermal Stability. Thermogravimetric behavior of acrylic resin and OPEFB fibers is shown in Table 1. The onset degradation for acrylic resin, defined by 50% weight loss, was linked to water evaporation followed by solvents and additives losing within the range of 40°C to 150°C. It was also observed the degradation of methylmethacrylate polymer chains due to

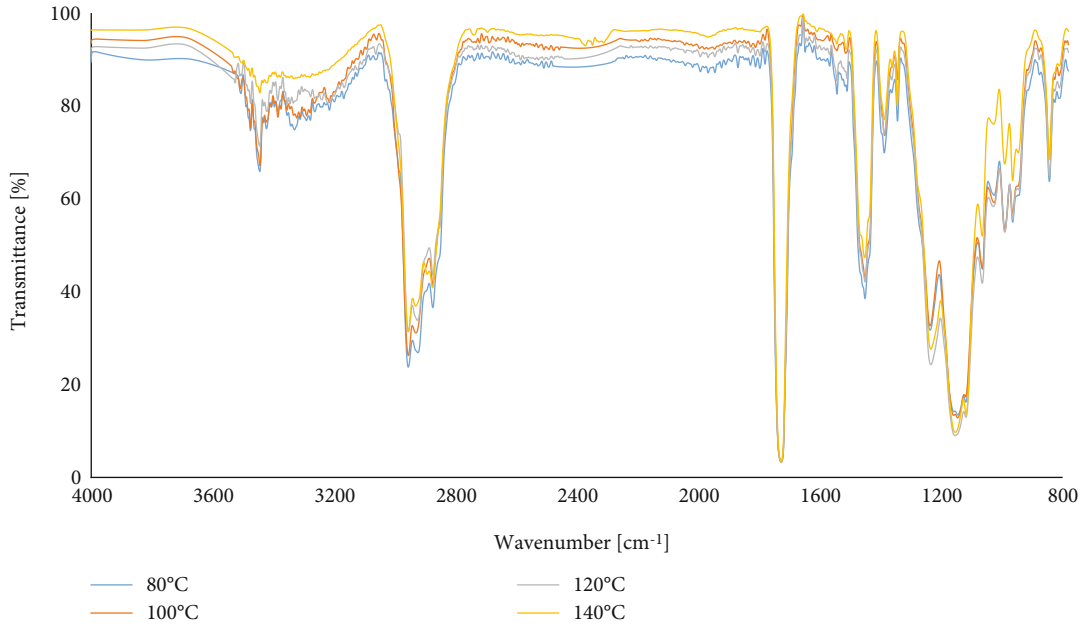

(a)

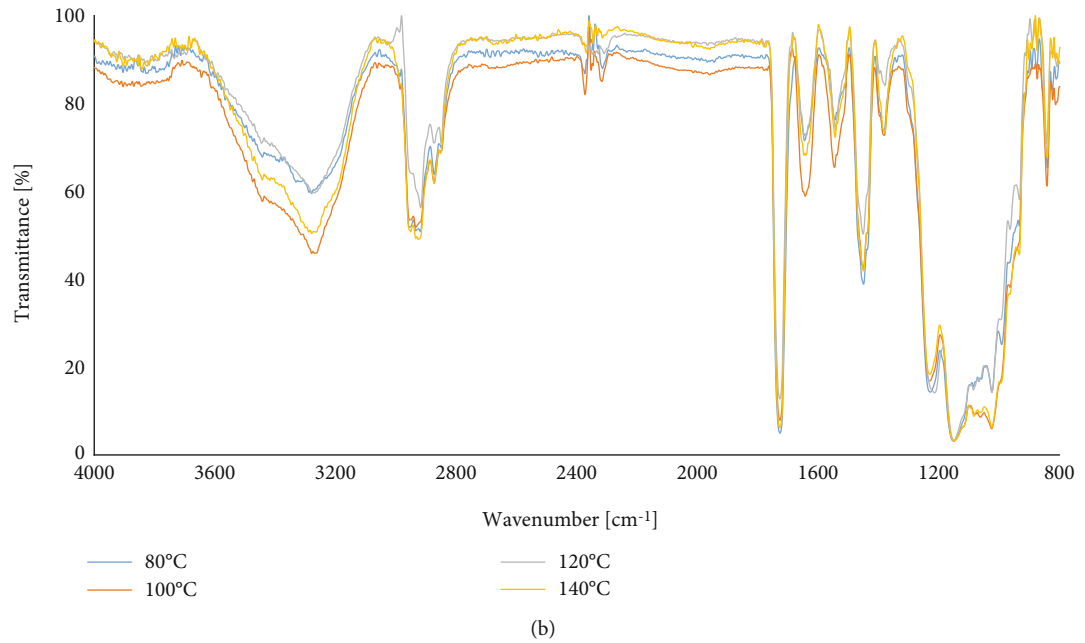

(b)

Figure 8: Continued.

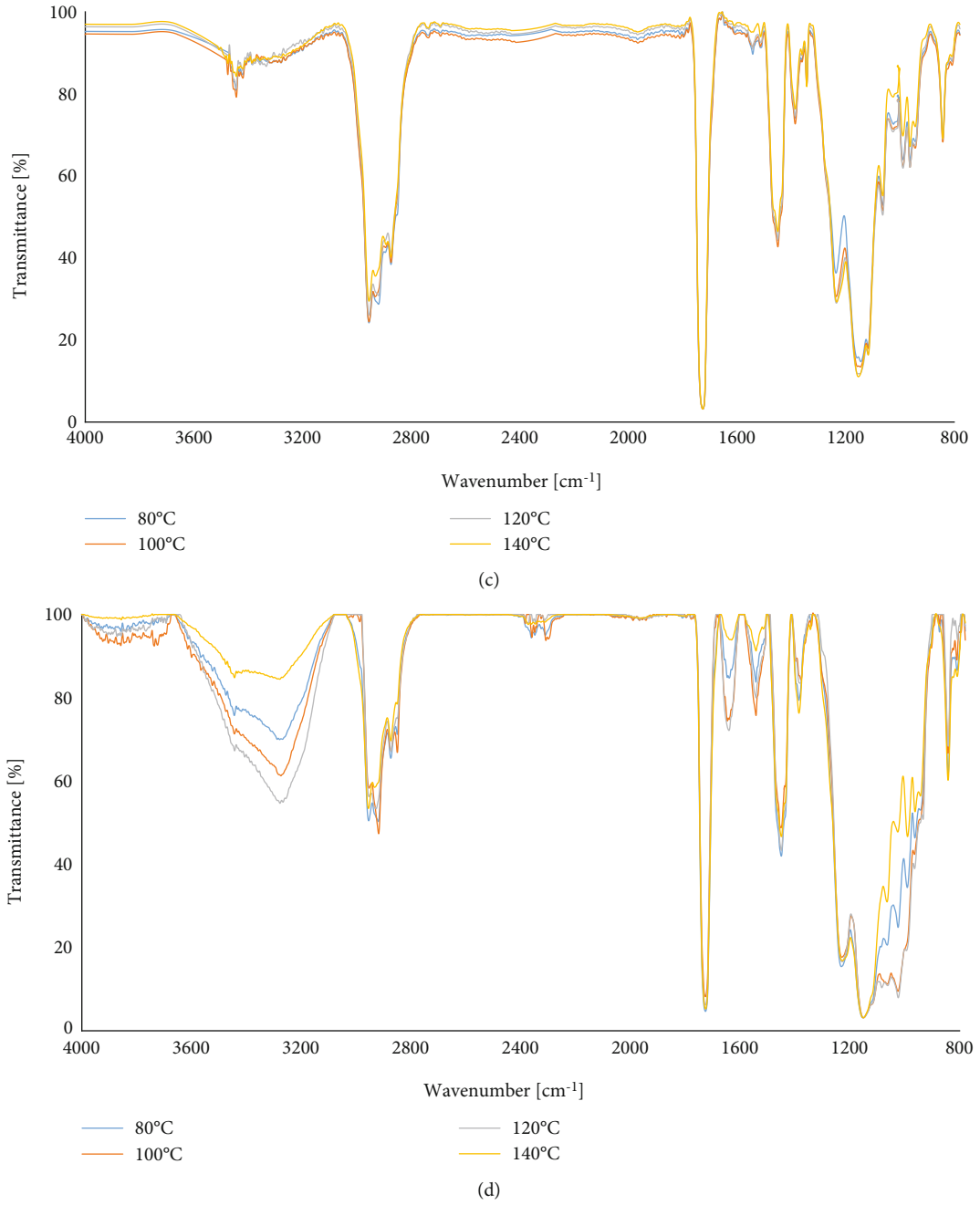

Figure 8: FTIR curves of OPEFB/acrylic thermoplastic composites (a) before aging—605 μm, (b) after aging—605 μm, (c) before aging—633 μm, and (d) after aging—633 μm.

Table 1: Thermogravimetric results of raw materials at different decomposition stages.

Raw material	Weight loss (%)/temperature range (°C)			
	First stage	Second stage	Third stage	Fourth stage
OPEFB (fibers)	8.03/20-150	59.93/150-460	4.60/460-600	-
Acrylic resin (aqueous emulsion)	18.95/40-75	11.20/76-95	20.17/96-150	48.35/151-600

unzipping reactions. This step involved nearly a 48% weight loss, and it was produced over 150°C. As regards OPEFB fibers, losing of free water and volatiles were produced in the range of 20°C to 150°C after which, it was evidenced the highest degradation process. This stage was observed from 150°C to 460°C and corresponded to the degradation of pectin, hemicellulose, cellulose, and lignin as well as to organic extractives decompose [68].

Thermal degradation mechanisms are narrowly related with the microstructure of lignocellulosic fibers. In a broad

Table 2: Thermogravimetric results of OPEFB/acrylic thermoplastic composites.

Fiber size (μm)	Processing temperature (°C)	Weight loss before aging (%)		Weight loss after aging (%)	
		First stage 24-224°C	Second stage 225-600°C	First stage 24-216°C	Second stage 217-600°C
605	80	2.78	87.02	1.77	86.88
	100	2.17	88.92	2.42	84.09
	120	2.05	86.68	2.28	85.02
	140	2.53	86.36	2.18	85.39
633	80	2.79	82.45	2.88	84.00
	100	2.42	81.87	2.57	81.78
	120	2.34	84.24	3.10	84.99
	140	2.57	83.86	2.92	83.04

sense, cellulose comprises sequences of both crystalline and amorphous regions. Cellulose structure is composed with β (1-4)-linked D-glucose units that are intimately connected and periodically ordered in three-dimensional disposition. On the contrary, hemicellulose contains non-crystalline regions which are easily hydrolysable. Although cellulose and hemicellulose show significative differences, important interactions are produced between them. It has been proposed that shear forces between cellulose fibril surface and hemicellulose are generated through the interactions of hemicellulose side groups with the free hydroxyl groups of the cellulose [69, 70]. Initial thermal decomposition takes place in amorphous structure of cellulose, hemicellulose, and lignin, followed by degradation of cellulose crystalline segments [71]. Intermolecular hydrogen bonds of cellulose generate tertiary fibrillar structures of high crystallinity requiring more heat for thermal degradation [72]. In this regard, thermal results of OPEFB were found to be in good agreement with a previous study [37].

As can be seen in Table 2, thermogravimetric results of composites showed different degradation patterns to the pristine materials. Considering morphologic aspects of imbibed fibers presented in Figures 2(a) and 2(b) and overall thermal results, it is noticed that the incorporation of OPEFB into acrylic matrix increased thermal stability of the system. Specifically, results revealed two weight loss zones between 30°C and 600°C. The first step, with approximately 3% weight loss, was ascribed to the evaporation of solvents and residual water [73]. The second stage exhibited the highest weight loss (85%) due to a number of different degradation mechanisms associated, as aforementioned, to decomposition stages of cellulose, hemicellulose, and lignin. In addition, processes with greater activation energy like main-chain and side-group scissions as well as depolymerization were produced in the second step [74]; typically, carbon-hydrogen, carbon-hydrogen, carbon-oxygen, carbon-carbon, and hydrogen-oxygen bonds are broken with energy requirements ranging from 340 to 460 kJ/mol [73].

Regarding fiber size and processing temperature, there were relatively minor differences in composites elaborated with fibers sized 605 and 633 μm. This behavior was similar in the case of processing temperatures. Literature surveys focused on TGA of natural fiber-reinforced thermoplastic polymer composites showed somewhat similar results to the present study [75, 76]; nevertheless, those studies are not conducted with OPEFB fibers and acrylic thermoplastic polymer as matrix.

Based on the results after aging, it is also evident minor quantitative differences in thermal degradation of OPEFB/acrylic thermoplastic composites. Even though SEM micrographs of Figure 4 evidenced some biodegradation signals, they seem not to have important effects on thermogravimetric behavior of the composites. At this stage of the investigation, physicochemical characteristics of OPEFB fibers, fungal, voids, and microcracks produced weight loss differences among formulations, which are considered to be within the variation expected experimentally. On the other hand, the degradation of raw materials can produce undesirable effects on the thermal stability; however, the manufacture of studied composites requires the mixing of fibers and matrix at temperatures under 150°C. Notice that extensive degradation of composite took place before and after aging process, over 200°C. Therefore, these differences are not considered, from a practical significance, as important decomposition patterns.

4. Conclusions

The salt fog spray aging of acrylic thermoplastic composites reinforced with OPEFB fiber was investigated at different processing temperatures and fiber sizes to better understand potentiality of both waterborne acrylic matrix and OPEFB wastes. For all composites, it was observed detectable levels of *Aspergillus* spp. of fungi after salt spray testing as a result of biodegradation of lignin, cellulose, and hemicellulose. SEM analysis showed random orientation microstructural defects like voids and microcracks in the composites. Mechanical behavior of composites turned out to be dominated by the processing temperature and fiber size. Although some nonhomogeneous variations in tensile properties at different fiber sizes and processing temperatures were observed, overall results evidenced a positive balance of tensile performance with the processing temperature increase. On the other hand, FTIR results showed important bands associated to carboxylic acids, phenolic compounds, carbon dioxide, and amides that confirmed fungal growth. TGA results showed two degradation stages almost constant for all specimens, and no significant influence of processing temperature and fiber size was observed. Furthermore, aging with salt spray atmosphere did not affect thermal stability of composites at this research stage. The findings and observations of this research lead to further understanding of OPEFB fiber-reinforced acrylic matrix composites. Such knowledge is essential for highlighting applications where obtained composite would most effectively be employed and may provide guidance on necessary performance enhancing modification for future industrial scale up.

Data Availability

There is no extra data supporting the results.

Conflicts of Interest

The authors declare that they have no conflicts of interest.

Acknowledgments

The authors gratefully acknowledge the financial support provided by the Escuela Politécnica Nacional, for the development of the Project PIGR-19-10: "Aprovechamiento de desechos industriales de aceite de palma africana en el desarrollo de polímeros compostables, composites y sistemas de biofiltración."

References

[1] N. A. Nordin, N. M. M. A. Rahman, and A. Hassan, "Conditioning effect on the mechanical and thermal properties of

heat-treated oil palm empty fruit bunch/high-density polyethylene composite," *High Performance Polymers*, vol. 32, no. 2, pp. 158–167, 2020.

[2] H. Awais, Y. Nawab, A. Amjad, A. Anjang, H. Akil, and M. S. Zainol, "Environmental benign natural fibre reinforced thermoplastic composites: a review," *Composites Part C: Open Access*, vol. 4, p. 100082, 2021.

[3] W. Chaiwong, N. Samoh, T. Eksomtramage, and K. Kaewtatip, "Surface-treated oil palm empty fruit bunch fiber improved tensile strength and water resistance of wheat gluten-based bioplastic," *Composites Part B: Engineering*, vol. 176, p. 107331, 2019.

[4] C. S. Hassan, P. Qiang, S. M. Sapuan, A. A. Nuraini, M. Y. M. Zuhri, and R. A. Ilyas, "Unidirectional oil palm empty fruit bunch (OPEFB) fiber reinforced epoxy composite car bumper beam—effects of different fiber orientations on its crash performance," *Biocomposite and Synthetic Composites for Automotive Applications*, pp. 233–253, 2021.

[5] J. O. Akindoyo, M. D. H. Beg, S. Ghazali, H. P. Heim, M. Feldmann, and M. Mariatti, "Oxidative induction and performance of oil palm fiber reinforced polypropylene composites – effects of coupling agent and UV stabilizer," *Composites Part A: Applied Science and Manufacturing*, vol. 125, p. 105577, 2019.

[6] N. A. Latip, A. H. Sofian, M. F. Ali, S. N. Ismail, and D. M. N. D. Idris, "Structural and morphological studies on alkaline pre-treatment of oil palm empty fruit bunch (OPEFB) fiber for composite production," *Materials Today: Proceedings*, vol. 17, pp. 1105–1111, 2019.

[7] N. A. Ramlee, M. Jawaid, E. S. Zainudin, and S. A. K. Yamani, "Tensile, physical and morphological properties of oil palm empty fruit bunch/sugarcane bagasse fibre reinforced phenolic hybrid composites," *Journal of Materials Research and Technology*, vol. 8, no. 4, pp. 3466–3474, 2019.

[8] N. Saba, M. Jawaid, O. Y. Alothman, and Z. Almutairi, "Evaluation of dynamic properties of nano oil palm empty fruit bunch filler/epoxy composites," *Journal of Materials Research and Technology*, vol. 8, no. 1, pp. 1470–1475, 2019.

[9] R. Santiagoo, N. Kasmuri, S. Ramasamy, R. Ahmad, A. A. Ghani, and N. Zahari, "Characterization and comparison of oil palm empty fruit bunch fiber composite with and without stearic acid as compatibilizer in polypropylene/recycled acrylonitrile butadiene rubber matrices," *PROCEEDINGS OF 8TH INTERNATIONAL CONFERENCE ON ADVANCED MATERIALS ENGINEERING & TECHNOLOGY (ICAMET 2020)*, vol. 2347, 2021.

[10] D. Y. S. Low, J. Supramaniam, A. h. b. a. Rahim, S. y. Tang, and B. F. Leo, "Morphological, thermal, and mechanical properties of natural rubber reinforced with cellulose nanofibers from oil palm empty fruit bunch," *Journal of Rubber Research*, vol. 24, no. 4, pp. 631–640, 2021.

[11] T. H. Mokhothu and M. J. John, "Review on hygroscopic aging of cellulose fibres and their biocomposites," *Carbohydrate Polymers*, vol. 131, pp. 337–354, 2015.

[12] A. Chilali, M. Assarar, W. Zouari, H. Kebir, and R. Ayad, "Effect of geometric dimensions and fibre orientation on 3D moisture diffusion in flax fibre reinforced thermoplastic and thermosetting composites," *Composites. Part A, Applied Science and Manufacturing*, vol. 95, pp. 75–86, 2017.

[13] J. Koleske, "Paint and Coating Testing Manual," in *15th. Edition of the Gardner-Sward Handbook*, West Conshohocken, PA, ASTM International, 2012.

[14] N. Han, I. Baran, J. S. M. Zanjani, O. Yuksel, L. L. An, and R. Akkerman, "Experimental and computational analysis of the polymerization overheating in thick glass/Elium® acrylic thermoplastic resin composites," *Composites. Part B, Engineering*, vol. 202, p. 108430, 2020.

[15] W. Obande, D. Mamalis, D. Ray, L. Yang, and C. M. Ó. Brádaigh, "Mechanical and thermomechanical characterisation of vacuum-infused thermoplastic- and thermoset-based composites," *Materials & Design*, vol. 175, 2019.

[16] G. Kinvi-Dossou, R. M. Boumbimba, N. Bonfoh et al., "Innovative acrylic thermoplastic composites versus conventional composites: improving the impact performances," *Composite Structures*, vol. 217, 2019.

[17] S. Z. H. Shah, P. S. M. Megat-Yusoff, S. Karuppanan et al., "Performance comparison of resin-infused thermoplastic and thermoset 3D fabric composites under impact loading," *International Journal of Mechanical Sciences*, vol. 189, p. 105984, 2021.

[18] T. Pini, F. Briatico-Vangosa, R. Frassine, and M. Rink, "Matrix toughness transfer and fibre bridging laws in acrylic resin based CF composites," *Engineering Fracture Mechanics*, vol. 203, pp. 115–125, 2018.

[19] G. Gohel, S. K. Bhudolia, S. B. S. Elisetty, K. F. Leong, and P. Gerard, "Development and impact characterization of acrylic thermoplastic composite bicycle helmet shell with improved safety and performance," *Composites. Part B, Engineering*, vol. 221, p. 109008, 2021.

[20] L. C. M. Barbosa, D. B. Bortoluzzi, and A. C. Ancelotti, "Analysis of fracture toughness in mode II and fractographic study of composites based on Elium® 150 thermoplastic matrix," *Composites. Part B, Engineering*, vol. 175, p. 107082, 2019.

[21] M. E. Kazemi, L. Shanmugam, S. Chen, L. Yang, and J. Yang, "Novel thermoplastic fiber metal laminates manufactured with an innovative acrylic resin at room temperature," *Composites Part A: Applied Science and Manufacturing*, vol. 138, 2020.

[22] D. Mamalis, W. Obande, V. Koutsos, J. R. Blackford, C. M. Ó. Brádaigh, and D. Ray, "Novel thermoplastic fibre-metal laminates manufactured by vacuum resin infusion: the effect of surface treatments on interfacial bonding," *Materials and Design*, vol. 162, pp. 331–344, 2019.

[23] L. Shanmugam, M. E. Kazemi, Z. Rao et al., "Enhanced mode I fracture toughness of UHMWPE fabric/thermoplastic laminates with combined surface treatments of polydopamine and functionalized carbon nanotubes," *Composites. Part B, Engineering*, vol. 178, p. 107450, 2019.

[24] M. E. Kazemi, L. Shanmugam, Z. Li, R. Ma, L. Yang, and J. Yang, "Low-velocity impact behaviors of a fully thermoplastic composite laminate fabricated with an innovative acrylic resin," *Composite Structures*, vol. 250, 2020.

[25] P. Khalili, R. Kádár, M. Skrifvars, and B. Blinzler, "Impregnation behaviour of regenerated cellulose fabric Elium® composite: experiment, simulation and analytical solution," *Journal of Materials Research and Technology*, vol. 10, pp. 66–73, 2021.

[26] M. E. Kazemi, L. Shanmugam, D. Lu, X. Wang, B. Wang, and J. Yang, "Mechanical properties and failure modes of hybrid fiber reinforced polymer composites with a novel liquid thermoplastic resin, Elium®," *Composites. Part A, Applied Science and Manufacturing*, vol. 125, 2019.

[27] M. Haggui, A. El Mahi, Z. Jendli, A. Akrout, and M. Haddar, "Static and fatigue characterization of flax fiber reinforced thermoplastic composites by acoustic emission," *Applied Acoustics*, vol. 147, pp. 100–110, 2019.

[28] S. Samal, M. Stuchlík, and I. Petrikova, "Thermal behavior of flax and jute reinforced in matrix acrylic composite," *Journal of Thermal Analysis and Calorimetry*, vol. 131, no. 2, pp. 1035–1040, 2018.

[29] C. Baley, M. Lan, A. Bourmaud, and A. Le Duigou, "Compressive and tensile behaviour of unidirectional composites reinforced by natural fibres: influence of fibres (flax and jute), matrix and fibre volume fraction," *Materials Today Communications*, vol. 16, pp. 300–306, 2018.

[30] P. Khalili, B. Blinzler, R. Kádár et al., "Ramie fabric Elium® composites with flame retardant coating: flammability, smoke, viscoelastic and mechanical properties," *Composites. Part A, Applied Science and Manufacturing*, vol. 137, 2020.

[31] S. H. Ahmed and W. M. Salih, "Mechanical properties of acrylic laminations resin (PMMA) reinforced by natural nanoparticles and hemp fibers," *IOP Conference Series: Materials Science and Engineering*, vol. 1094, no. 1, 2021.

[32] E. I. Akpan, B. Wetzel, and K. Friedrich, "A fully biobased tribology material based on acrylic resin and short wood fibres," *Tribology International*, vol. 120, pp. 381–390, 2018.

[33] D. G. Weldon, "Failure analysis of paints and coatings: revised edition," *Fail. Anal. Paint. Coatings Revis. Ed.*, pp. 1–362, 2009.

[34] J. A. Nixon, "9-Vacuum Infusion: Cost-effective Closed Mould Processing to Meet the Challenges of the Styrene Issue," in *Integrated Design and Manufacture Using Fibre-Reinforced Polymeric Composites*, M. J. Owen, V. Middleton, and I. A. Jones, Eds., pp. 125–139, Woodhead Publishing, 2000.

[35] C. J. G. Plummer, P.-E. Bourban, and J.-A. Månson, "Polymer Matrix Composites: Matrices and Processing," in *Reference Module in Materials Science and Materials Engineering*, pp. 1–9, 2016.

[36] O. Ø. Knudsen and A. Forsgren, *Corrosion Control through Organic Coatings*, CRC Press, Second Edition edition, 2017.

[37] V. Valle, P. Baquero, P. Rico, J. Kreiker, B. Raggiotti, and F. Cadena, "Mechanical characteristics of composites based on oil palm empty fruit bunch, modified oca starch and polyvinyl alcohol," *Journal of Composite Materials*, vol. 55, no. 18, pp. 2459–2468, 2021.

[38] S. Y. Fu, B. Lauke, and Y. W. Mai, Eds., *Science and Engineering of Short Fibre-Reinforced Polymer Composites, Second*, Elsevier, Duxford, 2019.

[39] K. K. Chawla, Ed., *Composite Materials: Science and Engineering, Fourth*, Springer, Cham, 2019.

[40] K. L. Goh, M. K. Aswathi, R. T. SilvaDe, and S. Thomas, Eds., *Interfaces in Particle and Fibre Reinforced Composites: Current Perspectives on Polymer, Ceramic, Metal and Extracellular Matrices, First*, Elsevier, Duxford, 2020.

[41] A. A. Tahir, N. F. Mohd Barnoh, N. Yusof et al., "Microbial diversity in decaying oil palm empty fruit bunches (OPEFB) and isolation of lignin-degrading bacteria from a tropical environment," *Microbes and Environments*, vol. 34, no. 2, pp. 161–168, 2019.

[42] A. Vashishtha and G. K. Meghwanshi, "Fungi inhabiting in hypersaline conditions: an insight," *Fungi and their Role in Sustainable Development: Current Perspectives*, pp. 449–465, 2018.

[43] A. N. Yadav, T. Kaur, D. Kour et al., *Saline Microbiome: Biodiversity, Ecological Significance, and Potential Role in Amelioration of Salt Stress*, Elsevier Inc., 2020.

[44] R. Rahman and S. Z. F. S. Putra, *Tensile Properties of Natural and Synthetic Fiber-Reinforced Polymer Composites*, Elsevier Ltd, 2019.

[45] W. Obande, C. M. Ó. Brádaigh, and D. Ray, "Continuous fibre-reinforced thermoplastic acrylic-matrix composites prepared by liquid resin infusion – a review," *Composites Part B: Engineering*, vol. 215, 2021.

[46] A. Chilali, W. Zouari, M. Assarar, H. Kebir, and R. Ayad, "Analysis of the mechanical behaviour of flax and glass fabrics-reinforced thermoplastic and thermoset resins," *Journal of Reinforced Plastics and Composites*, vol. 35, no. 16, pp. 1217–1232, 2016.

[47] M. Jawaid, P. M. Tahir, and N. Saba, Eds., *Lignocellulosic Fibre and Biomass-Based Composite Materials: Processing, Properties and Applications, First*, Elsevier, Duxford, 2017.

[48] M. R. M. Asyraf, M. R. Ishak, A. Syamsir et al., "Mechanical properties of oil palm fibre-reinforced polymer composites: a review," *Journal of Materials Research and Technology*, vol. 17, pp. 33–65, 2022.

[49] R. Kumar, M. I. Ul Haq, A. Raina, and A. Anand, "Industrial applications of natural fibre-reinforced polymer composites – challenges and opportunities," *International Journal of Sustainable Engineering*, vol. 12, no. 3, pp. 212–220, 2019.

[50] M. S. Sreekala, M. G. Kumaran, S. Joseph, M. Jacob, and S. Thomas, "Oil palm fibre reinforced phenol formaldehyde composites: influence of fibre surface modifications on the mechanical performance," *Appl. Compos. Mater*, vol. 7, no. 5, pp. 295–329, 2000.

[51] M. N. K. Chowdhury, M. D. H. Beg, M. R. Khan, and M. F. Mina, "Modification of oil palm empty fruit bunch fibers by nanoparticle impregnation and alkali treatment," *Cellulose*, vol. 20, no. 3, pp. 1477–1490, 2013.

[52] M. K. Faizi, "Tensile characterizations of oil palm empty fruit bunch (OPEFB) fibres reinforced composites in various epoxy/fibre fractions," *Biointerface Research in Applied Chemistry*, vol. 12, no. 5, pp. 6148–6163, 2022.

[53] W. P. Limited, *Natural Fibre Composites Materials, Processes and Properties*, Woodhead Publishing Limited, Philadelphia, 2014.

[54] H. Mohit and V. A. M. Selvan, "A comprehensive review on surface modification, structure interface and bonding mechanism of plant cellulose fiber reinforced polymer based composites," *Composite Interfaces*, vol. 25, no. 5–7, pp. 629–667, 2018.

[55] J. F. Wong, A. Hassan, J. X. Chan, and S. M. Kabeb, *Plastics in Corrosion Resistant Applications*, Elsevier, Reference Module in Materials Science and Materials Engineering, 2020.

[56] M. Falkiewicz-Dulik, K. Janda, and G. Wypych, Eds., *Handbook of Material Biodegradation, Biodeterioration, and Biostablization, Second*, Elsevier, Toronto, 2015.

[57] P. K. Mallick, *Fiber-Reinforced Composites*, CRC Press Taylor & Francis Group, 2007.

[58] B. H. Stuart, *Infrared Spectroscopy: Fundamentals and Applications*, 2005.

[59] S. Zakaria, H. Hamzah, J. A. Murshidi, and M. Deraman, "Chemical modification on lignocellulosic polymeric oil palm empty fruit bunch for advanced material," *Advances in Polymer Technology*, vol. 20, no. 4, 2001.

[60] M. A. Abdullah, M. S. Nazir, M. R. Raza, B. A. Wahjoedi, and A. W. Yussof, "Autoclave and ultra-sonication treatments of oil palm empty fruit bunch fibers for cellulose extraction and

its polypropylene composite properties," *Journal of Cleaner Production*, vol. 126, pp. 686–697, 2016.

[61] C. A. Kakou, F. Z. Arrakhiz, A. Trokourey, R. Bouhfid, A. Qaiss, and D. Rodrigue, "Influence of coupling agent content on the properties of high density polyethylene composites reinforced with oil palm fibers," *Materials and Design*, vol. 63, pp. 641–649, 2014.

[62] P. Khalili, K. Y. Tshai, and I. Kong, "Comparative thermal and physical investigation of chemically treated and untreated oil palm EFB fiber," *Materials Today: Proceedings*, vol. 5, no. 1, pp. 3185–3192, 2018.

[63] N. S. Rosli, S. Harun, J. M. Jahim, and R. Othaman, "Chemical and physical characterization of oil palm empty fruit bunch," *Malaysian Journal of Analytical Sciences*, vol. 21, no. 1, pp. 188–196, 2017.

[64] W. P. Limited, *Handbook of Natural Fibres Volume 1: Types, Properties and Factors Affecting Breeding and Cultivation*, Woodhead Publishing Limited, Philadelphia, 2012.

[65] S. Palamae, P. Dechatiwongse, W. Choorit, Y. Chisti, and P. Prasertsan, *Cellulose and hemicellulose recovery from oil palm empty fruit bunch (EFB) fibers and production of sugars from the fibers*, vol. 155, Elsevier Ltd., 2017.

[66] E. Hoffland, T. W. Kuyper, H. Wallander et al., "The role of fungi in weathering in a nutshell," *Frontiers in Ecology and the Environment*, vol. 2, no. 5, pp. 258–264, 2004.

[67] R. Bhat, "Potential use of fourier transform infrared spectroscopy for identification of molds capable of producing mycotoxins," *International Journal of Food Properties*, vol. 16, no. 8, pp. 1819–1829, 2013.

[68] S. H. Chang, "An overview of empty fruit bunch from oil palm as feedstock for bio-oil production," *Biomass and Bioenergy*, vol. 62, pp. 174–181, 2014.

[69] G. Brunner, *Processing of Biomass with Hydrothermal and Supercritical Water*, vol. 5, 2014.

[70] A. Khodayari, W. Thielemans, U. Hirn, A. W. Van Vuure, and D. Seveno, "Cellulose-hemicellulose interactions - a nanoscale view," *Carbohydrate Polymers*, vol. 270, 2021.

[71] M. A. Norul Izani, M. T. Paridah, U. M. K. Anwar, M. Y. Mohd Nor, and P. S. H'Ng, "Affects of fiber treatment on morphology, tensile and thermogravimetric analysis of oil palm empty fruit bunches fibers," *Composites. Part B, Engineering*, vol. 45, no. 1, pp. 1251–1257, 2013.

[72] N. S. Hassan and K. H. Badri, "Thermal behaviors of oil palm empty fruit bunch fiber upon exposure to acid-base aqueous solutions," *Malaysian Journal of Analytical Science*, vol. 20, no. 5, pp. 1095–1103, 2016.

[73] J. D. Menczel and R. B. Prime, *Thermal Analysis of Polymers: Fundamentals and Applications*, 2009.

[74] H. M. Ng, N. M. Saidi, F. S. Omar, K. Ramesh, S. Ramesh, and S. Bashir, "Thermogravimetric Analysis of Polymers," *Encyclopedia of Polymer Science and Technology*, vol. 13, pp. 1–29, 2018.

[75] S. Krishnasamy, S. M. K. Thiagamani, C. M. Kumar et al., "Recent advances in thermal properties of hybrid cellulosic fiber reinforced polymer composites," *International Journal of Biological Macromolecules*, vol. 141, pp. 1–13, 2019.

[76] R. Wahab, S. M. M. Dom, M. T. Mustafa, H. W. Samsi, S. M. Rasat, and I. Khalid, "Properties of empty fruit bunch oil palm (Elaeis guineesis) composite boards at different densities and resin contents," *Journal of Plant Sciences*, vol. 10, no. 5, pp. 179–190, 2015.